

HAT-P-4b: A METAL-RICH LOW-DENSITY TRANSITING HOT JUPITER[†]

G. KOVÁCS¹, G. Á. BAKOS^{2,3}, G. TORRES², A. SOZZETTI^{2,4}, D. W. LATHAM², R. W. NOYES², R. P. BUTLER⁵,
 G. W. MARCY⁶, D. A. FISCHER⁷, J. M. FERNÁNDEZ², G. ESQUERDO², D. D. SASSELOV², R. P. STEFANIK², A. PÁL⁸,
 J. LÁZÁR⁹, I. PAPP⁹, & P. SÁRI⁹

Draft version October 23, 2018

ABSTRACT

We describe the discovery of HAT-P-4b, a low-density extrasolar planet transiting BD+36 2593, a $V = 11.2$ mag slightly evolved metal-rich late F star. The planet's orbital period is 3.056536 ± 0.000057 d with a mid-transit epoch of $2,454,245.8154 \pm 0.0003$ (HJD). Based on high-precision photometric and spectroscopic data, and by using transit light curve modeling, spectrum analysis and evolutionary models, we derive the following planet parameters: $M_p = 0.68 \pm 0.04 M_J$, $R_p = 1.27 \pm 0.05 R_J$, $\rho_p = 0.41 \pm 0.06 \text{ g cm}^{-3}$ and $a = 0.0446 \pm 0.0012$ AU. Because of its relatively large radius, together with its assumed high metallicity of that of its parent star, this planet adds to the theoretical challenges to explain inflated extrasolar planets.

Subject headings: planetary systems: individual: HAT-P-4b — stars: individual: BD+36 2593 — techniques: photometric — techniques: spectroscopic

1. INTRODUCTION

In the course of our ongoing wide field planetary transit search program HATNet (Bakos et al. 2004), we have discovered a large radius and low density planet orbiting an 11th magnitude star BD+36 2593. This planet is the fifth member of a group of low-density transiting exoplanets. The combination of its low mass and the relatively high metallicity and age of the parent star makes theoretical interpretation of its large radius difficult. In this Letter we describe the observational properties of the system and derive the physical parameters both for the host star and for the planet. We also briefly comment on the theoretical status of inflated extrasolar planets.

2. THE PHOTOMETRIC DISCOVERY AND FOLLOW-UP OBSERVATIONS

The star BD+36 2593 (also GSC 02569-01599) at $\alpha = 15^h 19^m 57^s.92$, $\delta = +36^\circ 13' 46''.7$, is contained in field G191 of HATNet, centered at $\alpha = 15^h 28^m$, $\delta = +37^\circ 30'$. As we show in the remainder of the paper, the star is orbited by a planetary companion, and so we label the host star as HAT-P-4 and the planet as HAT-P-4b. Field

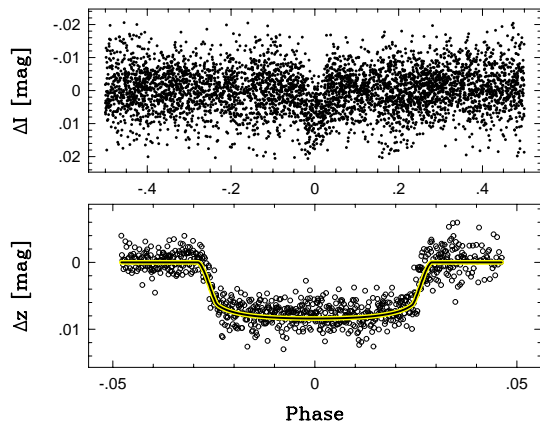


FIG. 1.— Folded and unbinned light curves of HAT-P-4. The HATNet and FLWO 1.2 m data are plotted in the upper and lower panels, respectively. The transit model fit to the FLWO data is shown by continuous line (see Table 3 for the resulting transit parameters). The out-of-transit level of the HATNet data corresponds to $I = 10.537$ mag, phase is zero at the transit center.

G191 was monitored from 2004 December until 2005 June by the HAT-7 telescope at the Fred Lawrence Whipple Observatory (FLWO) of the Smithsonian Astrophysical Observatory (SAO). Nearly 90% of the data points were gathered after February 2005. The field is relatively sparse, with ~ 14000 objects brighter than $I \approx 14$ mag. Most of the light curves have some 5300 data points. The sampling cadence is 5.5 min, slightly longer than the 5 min integration time.

A first look at the compact subset collected in the 98 d time span between March and June, 2005, revealed the presence of a transit signal with a nearly integer 3 d period. The detection was made possible by the application of the Trend Filtering Algorithm (TFA; Kovács, Bakos, & Noyes 2005). However, assuming the primary is a main-sequence F or G type star, the relative length of the transit is some 20 – 30% greater than expected for a Jupiter-size companion with the above orbital period. Although both the lack of detection in the

¹ Konkoly Observatory, Budapest, P.O. Box 67, H-1125, Hungary; kovacs@konkoly.hu

² Harvard-Smithsonian Center for Astrophysics (CfA), 60 Garden Street, Cambridge, MA 02138, USA

³ Hubble Fellow.

⁴ INAF - Osservatorio Astronomico di Torino, Strada Osservatorio 20, 10025, Pino Torinese, Italy

⁵ Department of Terrestrial Magnetism, Carnegie Institute of Washington DC, 5241 Broad Branch Rd. NW, Washington DC, USA 20015-1305

⁶ Department of Astronomy, University of California, Berkeley, CA 94720, USA

⁷ Department of Physics & Astronomy, San Francisco State University, San Francisco, CA 94132, USA

⁸ Department of Astronomy, Eötvös Loránd University, Budapest, Hungary

⁹ Hungarian Astronomical Association, Budapest, Hungary

[†] Based in part on observations obtained at the W. M. Keck Observatory, which is operated by the University of California and the California Institute of Technology. Keck time has been in part granted by NASA.

raw data and the length of the transit made us suspicious about the viability of this candidate, we left some room for the possibility that the primary was slightly evolved (an assumption that proved to be true in the subsequent investigations — see § 4). Therefore, we proceeded with rejection-mode spectroscopy, which showed no sign of radial velocity (RV) variation at the km s^{-1} level.

An improved reduction of all available frames of the field was completed by February 2007. In addition to using a new data pipeline that employs refined astrometry (Pál & Bakos 2006) and aperture photometry, we detrended the light curves before signal search with the aid of an External Parameter Decorrelation technique (EPD, see also Bakos et al. 2007). This technique utilizes the fact that various “external parameters” that are specific to the star, such as sub-pixel position on the frame, point spread function properties (e.g., width and elongation), or specific to the frame, such as telescope position, are correlated with the deviations of the star’s brightness from the median. The technique is optimal for stars that are otherwise non-variable most of the time (e.g. transit candidates). EPD derives the correlation between brightness deviations and the underlying external parameters, and subsequently corrects them for each individual star. This is different from what is done during the application of TFA, where we consider the full time history of the light variation and use the light curves to “cure themselves” by recognizing the hidden systematics in each other. The two methods are complementary and we use both (EPD followed by TFA). All these led to a powerful confirmation of the earlier detection.

The folded light curve constructed from the HAT-Net data is shown in the upper panel of Fig. 1. The best period was obtained from the BLS analysis (Kovács, Zucker, & Mazeh 2002) after applying TFA with some 700 template stars.¹¹ As seen, the transit is clearly visible in the light curve even though no binning was applied. There is no sign of periodic out-of-transit variation, indicating that this is a near “textbook” transit signal.

To update the photometric ephemeris and obtain a precise light curve for model fitting, we observed our target with KeplerCam on the 1.2m telescope at FLWO. We observed two full transits on May 24 and 27, 2007. The folded light curve in the Sloan z band for all 985 data points is shown in the lower panel of Fig. 1. The follow-up observations verify the discovery light curve and are accurate enough to make transit modeling possible.

3. THE SPECTROSCOPIC VERIFICATION AND EXCLUSION OF BLEND SCENARIOS

As mentioned in § 2, basic rejection mode spectroscopy to exclude stellar binary and certain blend types was already initiated after the first detection in the fall of 2005. By June 2006 we had collected 9 spectra with the CfA Digital Speedometer (DS; Latham 1992) on the FLWO 1.5 m telescope, covering a 45 \AA window centered at the Mg b triplet at 5187 \AA . We derived spectroscopic parameters by comparing the observed spectra against synthetic spectra, as described in detail by Torres et al. (2002). The initial stellar parameters from

¹¹ The EPD technique played the main role in the detection; TFA subsequently led to an increase of 20% in the signal-to-noise ratio.

TABLE 1
HIRES RELATIVE RADIAL VELOCITIES FOR HAT-P-4.

BJD (2,400,000+)	RV (m s^{-1})	σ_{RV} (m s^{-1})	O-C (m s^{-1})	Phase ^a
54186.98522	101.0	2.1	2.7	0.753
54187.11241	92.6	2.1	-2.6	0.794
54188.01160	-25.4	2.0	0.3	0.088
54188.07150	-35.8	2.0	-2.0	0.108
54189.00174	-28.1	2.2	-2.8	0.412
54189.08262	-13.9	2.0	-0.7	0.439
54189.13222	-3.1	3.3	2.3	0.455
54249.93769	-52.5	2.8	-3.6	0.349
54279.86357	-36.8	2.9	8.4	0.139

^a Relative to the center of transit.

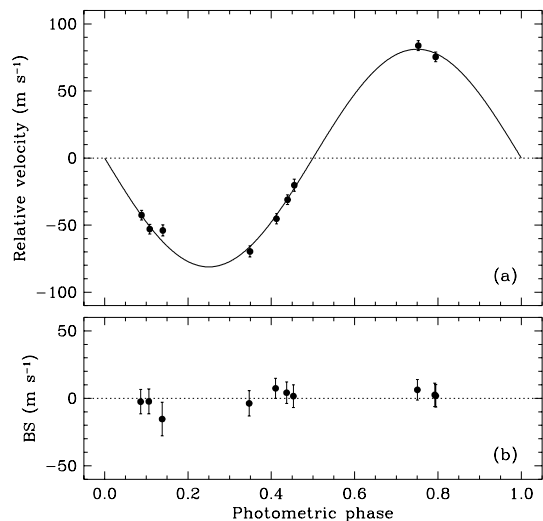


FIG. 2.— Relative radial velocity and bisector span variations from the Keck observations of HAT-P-4. Panel (a) shows the nine Keck RV measurements with a zero-eccentricity orbital fit. In panel (b) we show the bisector spans (from nine iodine exposures and one template spectrum) displaying a much smaller scatter. Error bars include the 3 m s^{-1} estimated velocity jitter.

this analysis were: $T_{\text{eff}} = 5500 \text{ K}$, $\log g = 3.5 [\text{cgs}]$ and $v \sin i = 5.9 \text{ km s}^{-1}$, indicating an evolved G-type primary¹². The DS spectra were also used to derive radial velocities by cross-correlating the spectra with synthetic spectra based on Kurucz model atmospheres (e.g. Latham 2002). The rms scatter of the RV data was 0.71 km s^{-1} around the mean velocity of -1.58 km s^{-1} . The velocities did not show any correlation with the orbital phase and we found no sign of a second stellar component in the spectra. These spectroscopic results, together with the secure detection in the HATNet data, made a viable case for obtaining high-precision RV measurements to seek evidence for orbital motion and to obtain refined stellar parameters. Accordingly, high-resolution spectroscopy was conducted with the HIRES instrument (Vogt et al. 1994) on the Keck I telescope between 2007 March 27 and May 29. See, e.g., Torres et al. (2007) for the details of the observational procedure. The

¹² These parameters were derived with $[\text{Fe}/\text{H}] = 0.0$. By using $[\text{Fe}/\text{H}] = 0.24$ from the Keck spectra we get a slightly better match with the synthetic spectra that yields $T_{\text{eff}} = 6000 \text{ K}$ and $\log g = 4.0$, in better agreement with the Keck results described below.

nine resulting RV measurements are listed in Table 1. They are relative RV velocities in the Solar System barycentric frame of reference (see Butler et al. 1996).

The data were fitted by a circular¹³ orbit with period and mid transit epoch constrained by the photometric data (see Table 3). The result of this two-parameter (systematic offset and semi-amplitude) fit is displayed in Fig. 2. The unbiased estimate of the standard deviation of the residuals is 4.1 m s^{-1} , larger than the internal errors listed in Table 1. A part of this scatter may come from the last data point that was taken under unfavorable weather conditions (leaving out this point we get 2.7 m s^{-1} for the standard deviation of the residuals). Nevertheless, it is also possible that there is a “velocity jitter” due to stellar activity. The size of this jitter is estimated to be about 3 m s^{-1} , falling in the expected range for an inactive late F-type star (Wright 2005). The low activity level is supported by the absence of emission features in the Ca II H and K lines.

A crucial part of the verification of the sub-stellar nature of the companion is testing various blend scenarios. There are at least two basic ways of such testing: (i) light curve modeling, combined with the information available from the spectra (e.g., maximum flux contribution by the blended binary); (ii) checking spectral line asymmetry by searching for bisector span variations (e.g., Santos et al. 2002; Torres et al. 2005). Our experience shows that while (i) requires several pieces of information (good quality full light curve, running many binary models and performing a fairly deep spectrum analysis), (ii) is more sensitive to hidden components and simpler to perform. Therefore, we settled on (ii) and searched for a variation in the differences measured between the velocities at the top and the bottom of the correlation profiles of the individual spectra. The result is shown in the lower panel of Fig. 2. For a hidden stellar binary blended by our target we would expect a variation in the bisector span in phase with the radial velocity, and with an amplitude comparable to that of the measured RV variation itself (Torres et al. 2005). However, the standard deviation of the bisector variation is 6.5 m s^{-1} , which is only 8% of the RV amplitude (the same numbers are 2.9 m s^{-1} and 4%, respectively, if we leave out the last data point). Furthermore, no correlation with the RV variation is seen. Therefore, we are confident that the source of the RV variation is stellar wobble due to the gravitational pull of a sub-stellar companion.

4. STELLAR AND PLANETARY PARAMETERS

The cornerstone of the derivation of the absolute parameters of a planet discovered by radial velocity and transit observations is the accurate estimation of the stellar mass and radius.

The procedure often involves determination of T_{eff} and $[\text{Fe}/\text{H}]$, as well as $\log g$, from high-resolution spectroscopic analysis. If an accurate distance is available, for example from a Hipparcos parallax, then the absolute magnitude can be used to improve the value for the stellar radius. In general, none of the methods yield better than $\sim 10\%$ accuracy in the derived stellar parameters (implying corresponding limits to the accuracy of

TABLE 2
STELLAR PARAMETERS FOR HAT-P-4.

Parameter	Value	Source
T_{eff} (K)	5860 ± 80	SME ^a
$[\text{Fe}/\text{H}]$ (dex)	$+0.24 \pm 0.08$	SME
$v \sin i$ (km s^{-1})	5.5 ± 0.5	SME
Mass (M_{\odot})	$1.26 [-0.14, 0.06]$	Y ² +LC+SME ^b
Radius (R_{\odot})	$1.59 [-0.07, 0.07]$	Y ² +LC+SME
$\log g$ (cgs)	$4.14 [-0.04, 0.01]$	Y ² +LC+SME
L_{\star} (L_{\odot})	$2.68 [-0.34, 0.39]$	Y ² +LC+SME
M_V (mag)	$3.74 [-0.16, 0.16]$	Y ² +LC+SME
Age (Gyr)	$4.2 [-0.6, 2.6]$	Y ² +LC+SME
Distance (pc)	310 ± 30	from M_V ^c

^a SME = “Spectroscopy Made Easy” package to generate synthetic spectra and to fit the observed ones (Valenti & Piskunov 1996).

^b Y²+LC+SME = Yonsei-Yale isochrones (Demarque et al. 2004), transit light curve modeling and SME analysis.

^c Using $V = 11.22 \pm 0.12$ of Droege (2006) and assuming zero reddening.

the absolute planet parameters). An improvement can be achieved by using the value of a/R_{\star} derived from the transit light curve to measure directly the mean stellar density (Sozzetti et al. 2007). Since this latter parameter is directly linked to $\log g$, entering in the spectroscopic analysis, we followed an iterative determination of the stellar and planetary parameters.

First, for the determination of $[\text{Fe}/\text{H}]$ and T_{eff} , we used the iodine-free template spectrum from Keck. The modeling was performed using the SME software (Valenti & Piskunov 1996) incorporating the same method and atomic data as given in Valenti & Fischer (2005). We obtained $T_{\text{eff}} = 6032 \pm 80 \text{ K}$, $[\text{Fe}/\text{H}] = +0.32 \pm 0.08$ [dex] and $\log g = 4.36 \pm 0.11$.

Next, for the computation a/R_{\star} , we fitted the high precision KeplerCam light curve (see Fig. 1) by using the formulae of Mandel & Agol (2002) with quadratic limb darkening coefficients from Claret (2004). We set $e = 0.0$ as a result of our test on the RV data with non-zero eccentricity. Fitted parameters were the center of transit T_c , the radius ratio R_p/R_{\star} , the normalized relative semi-major axis a/R_{\star} , and the impact parameter b .

Next, to compute the stellar mass and radius we relied on current stellar evolution models. As in our earlier papers, we compared the observational properties of the host star with a finely interpolated grid of model isochrones from Demarque et al. (2004). The inferred stellar properties are based on the best match to the measured values of T_{eff} , $[\text{Fe}/\text{H}]$, and a/R_{\star} within their observational errors, in a χ^2 sense. This procedure led to a better approximation of the stellar gravitational acceleration with $\log g = 4.12 \pm 0.04$.

In the second loop of iteration we used the newly determined value of $\log g$ in the SME analysis and redid the above sequence of computation. This led to a slightly modified set of stellar and planetary parameters with somewhat smaller errors than in the first loop. Since the changes were, in general, fairly small (e.g., $\log g$ has changed to 4.14 ± 0.03), we decided to stop the iteration after this second loop. The final stellar and planetary parameters are shown in Table 2 and Table 3, respectively.

Concerning the derived parameters and their errors,

¹³ A fit with free-floating eccentricity yields $e = 0.055 \pm 0.035$, supporting the assumption of a circular orbit.

TABLE 3
SPECTROSCOPIC, LIGHT CURVE AND PLANET
PARAMETERS OF HAT-P-4

Parameter	Value
Spectroscopic parameters:	
Period (d) ^a	3.056536 ± 0.000057
T _c (HJD) ^a	2,454,245.8154 ± 0.0003
	2,454,248.8716 ± 0.0006
<i>K</i> (m s ⁻¹)	81.1 ± 1.9
Offset velocity (m s ⁻¹) ^b .	12.1 ± 0.9
<i>e</i> ^c	0.0
Light curve parameters:	
Transit duration (day)...	0.1760 ± 0.0003
<i>a</i> / <i>R</i> _★	6.04 [-0.18, 0.03]
<i>R</i> _p / <i>R</i> _★	0.08200 ± 0.00044
<i>b</i> ≡ <i>a</i> cos <i>i</i> / <i>R</i> _★	0.01 [-0.01, 0.23]
Planet parameters:	
<i>M</i> _p (<i>M</i> _J)	0.68 ± 0.04
<i>R</i> _p (<i>R</i> _J)	1.27 ± 0.05
<i>ρ</i> _p (g cm ⁻³)	0.41 ± 0.06
log <i>g</i> _p (cm s ⁻²)	3.02 ± 0.02
<i>a</i> (AU)	0.0446 ± 0.0012
<i>i</i> _p (deg)	89.9° [-2.2, 0.1]

^a Taken from the photometry (HATNet and 2 nights of FLWO 1.2 m).

^b The γ velocity is -1.58 ± 0.24 km s⁻¹, from the DS data.

^c Adopted

we note the following. The dependence of the result on the evolutionary models was tested by using the isochrones given for solar-scaled $Z = 0.03$ models with core overshooting by Pietrinferni et al. (2006). As noted by the authors, their models are hotter by some 200 K than those of Demarque et al. (2004). Therefore, we used an effective temperature of 6060 K. With these input parameters we got nearly the same stellar and planet parameters as from the Yonsei-Yale isochrones (i.e., $\rho_p = 0.41$ g cm⁻³, age = 4.5 Gyr). By using models without overshooting or of lower effective temperature, we got larger ages and also slightly larger densities, up to $\rho_p = 0.43$ g cm⁻³. The stability of the planet density is mainly related to the correlated change of stellar mass and radius when models or input parameters are changed. These age ranges and the derived metallicity fit reasonably to the relation recently given by Reid et al. (2007). We also note that the derived radius is 34% larger than the one corresponding to an unevolved main-sequence star. This explains the longer than expected transit duration by which we were puzzled at the early phase of the discovery.

5. DISCUSSION AND CONCLUSIONS

We presented the discovery data and derived the physical parameters of HAT-P-4b, an inflated planet orbiting BD+36 2593. Among the 20 transiting planets discovered so far, there are five with $\rho_p \lesssim 0.4$ g cm⁻³. All others have at least 50% higher densities. For ease of comparison, Table 4 lists the relevant properties of the five inflated planets. It is remarkable how similar these planets are (except for TrES-4 that has distinctively low density). With its Saffronov number of 0.036, HAT-P-4b belongs to the Class II planets according to the recent classification of Hansen & Barman (2007) and (together with TrES-4) further strengthens the mysterious dichotomy of the

TABLE 4
COMPARISON OF THE PROPERTIES OF INFLATED PLANETS.^a

Name	P (d)	a (AU)	M (<i>M</i> _J)	R (<i>R</i> _J)	ρ (CGS)	log <i>g</i> (CGS)
WASP-1b	2.52	0.038	0.87	1.40	0.39	3.04
HAT-P-4b	3.06	0.045	0.68	1.27	0.41	3.02
HD 209458b	3.53	0.045	0.64	1.32	0.35	2.96
TrES-4	3.55	0.049	0.84	1.67	0.22	2.87
HAT-P-1b	4.47	0.055	0.53	1.20	0.38	2.96

^a Data from Shporer et al. (2007), this paper, Burrows et al. (2007), Mandushev et al. (2007) and Winn et al. (2007). From top to bottom, metallicities for the parent stars are: 0.23 (Stempels et al. 2007), 0.24, 0.02 0.0 (adopted) and 0.13.

known transiting planets in this parameter. The parent star of HAT-P-4b is among the largest radii, largest mass, lowest gravity and highest metallicity transiting planet host stars.

Current models of irradiated giant planets are able to match the observed radii of most of the planets without invoking any additional heating mechanism. Higher metallicity cases, such as the present one, however, may pose problems (assuming that the planet and star have similar metallicities). More metals imply two opposite effects on the radius: (i) inflating it due to higher opacities in the envelope; (ii) shrinking it due to the higher molecular weight of the interior and the possible development of a large high density core. These effects have been discussed recently by Burrows et al. (2007). Since WASP-1b is similar in several aspects (i.e., irradiance, metallicity) to HAT-P-4b, we consider the coreless models of WASP-1b as shown in Fig. 7 of Burrows et al. (2007). It seems that HAT-P-4b can be fitted by near solar metallicity coreless models, assuming that its age is not too much greater than 4 Gyr. We also refer to the layered convective mechanism of Chabrier & Baraffe (2007) that gives an alternative explanation for planets with inflated radii.

We conclude that more definite statements on the relation of the observations and planet structure theories can be made only by reaching higher accuracy in the observed star/planet parameters. Nevertheless, HAT-P-4b (together with WASP-1b) does not seem to support the existence of a simple relation between host star metallicity and planet's core mass (see Guillot et al. 2006; Burrows et al. 2007).

Operation of the HATNet project is funded in part by NASA grant NNG04GN74G. Work by G. Á. B. was supported by NASA through Hubble Fellowship Grant HST-HF-01170.01-A. G. K. wishes to thank support from Hungarian Scientific Research Foundation (OTKA) grant K-60750. We acknowledge partial support from the Kepler Mission under NASA Cooperative Agreement NCC2-1390 (D. W. L., PI). G. T. acknowledges partial support from NASA Origins grant NNG04LG89G. The Keck Observatory was made possible by the generous financial support of the W. M. Keck Foundation. D. A. F is a Cottrell Science Scholar of the Research Corporation. We acknowledge support from NASA grant NNG05G164G to DAF.

REFERENCES

- Bakos, G. Á. et al. 2004, *PASP*, 116, 266
Bakos, G. Á. et al. 2007, *ApJ*, in press (arXiv:0705.0126v2)
Burrows, A., Hubeny, I., Budaj, J., & Hubbard, W. B., 2007, *ApJ*, 661, 502
Butler, R. P. et al. 1996, *PASP*, 108, 500
Chabrier, G. & Baraffe, I. 2007, *ApJ*, 661, L81
Claret, A. 2004, *A&A*, 428, 1001
Droege, T. F., Richmond, M. W., & Sallman, M. 2006, *PASP*, 118, 1666
Demarque, P., Woo, J.-H., Kim, Y.-C., & Yi, S. K. 2004, *ApJS*, 155, 667
Guillot, T. et al. 2006, *A&A*, 453, L21
Hansen, B. M. S. & Barman, T. 2007, *ApJ*, in press (arXiv:0706.3052v1)
Kovács, G., Zucker, S., & Mazeh, T. 2002, *A&A*, 391, 369
Kovács, G., Bakos, G. Á., & Noyes, R. W. 2005, *MNRAS*, 356, 557
Latham, D. W. 1992, *ASP Conf. Ser.* 32, Vol. 32, 110
Latham, D. W. et al. 2002, *AJ*, 124, 1144
Mandel, K., & Agol, E. 2002, *ApJ*, 580, L171
Mandushev, G. et al. 2007, *ApJ*, in press (arXiv:0708.0834v1)
Pál, A., & Bakos, G. Á. 2006, *PASP*, 118, 1474
Pietrinferni, A., Cassisi, S., Salaris, M. & Castelli, F. 2006, *ApJ*, 642, 797
Reid, I. N. et al. 2007, *ApJ*, 665, 767
Santos, N. C. et al. 2002, *A&A*, 392, 215
Shporer, A., Tamuz, O., Zucker, S., & Mazeh, T. 2007, *MNRAS*, in press (arXiv:astro-ph/0610556v2)
Sozzetti, A. et al. 2007, *ApJ*, 664, 119
Stempels, H. C. et al. 2007, *MNRAS*, in press (arXiv:0705.1677)
Torres, G., Neuhäuser, R., & Guenther, E. W. 2002, *AJ*, 123, 1701
Torres, G., Konacki, M., Sasselov, D. D., & Jha, S. 2005, *ApJ*, 619, 558
Torres, G. et al. 2007, *ApJ*, 666, L121
Valenti, J. A., & Piskunov, N. 1996, *A&AS*, 118, 595
Valenti, J. A., & Fischer, D. A. 2005, *ApJS*, 159, 141
Vogt, S. S., et al. 1994, *Proc. SPIE*, 2198, 362
Winn, J. N. et al. 2007, *AJ*, in press (arXiv:0707.1908v1)
Wright, J. T. 2005, *PASP*, 117, 657